Supplementary Information

Revolutionizing Sample Preparation: A Novel Autonomous Microfluidic Platform for Serial Dilution

Dries Vloemans, Alexander Pieters, Francesco Dal Dosso and Jeroen Lammertyn[*]

KU Leuven, Department of Biosystems - Biosensors Group, Willem de Croylaan 42, box 2428, 3001 Leuven, Belgium

SI.1 Static colorimetric measurements for evaluation of mixing efficiency

In advance of executing the dynamic fluorescent measurements, a colorimetric analysis method was preformed to evaluate the evolution of the color distribution through the different expansion chambers. This gave information about the minimum number of required chambers to generate a homogeneous solution. In particular, a 10 µL drop of blue-colored (1:20 diluted) distilled water was drawn at a constant flow rate of 10 µL/min (with syringe pump) through the microfluidic chip (with DF of 2, 5 or 10x) composing of 6 expansion chambers in the mixing unit. The color distribution of the sample and diluent liquid was imaged at high resolution (600 dpi) within each expansion chamber using a fi-65F flatbed scanner and associated PaperStream Capture software (Fujitsu, Japan). An in-house developed Matlab® (R2020a, The MathWorks Inc., USA) script was used to extract the RGB values and determine the color distribution within each chamber. The extracted data was compared with the values of a reference chip containing multiple individual expansion chambers which were prefilled with solutions of known DFs (1, 2, 3, 4, 5 and 10x) of the blue- and yellow-colored liquid. The same methodology was used to evaluate the effect of the applied flow rate on the mixing efficiency. Hereto, a dilution module with DF of 5 was run at different flow rates of 5, 10 and 20 µL/min.

To determine the number of required chambers to obtain a homogenous reagent mixture, the mean RGB color and distribution within each of the 6 chambers (Figure SI. 1a) were analyzed and compared with the reference data. For all DFs (2, 5 and 10x), large errors bars and/or a discrepancy with the reference value for the R and/or B values are observed in the first 2 chambers indicating improper mixing of the blue and yellow liquids (Figure SI. 1b). From chamber 3 onwards all RGB values are found to be in line with the reference values. This means that within a DF range of 1-10x at least 3 chambers are required to obtain homogeneous mixing.

In Figure SI. 1c, the mean RGB values and error bars of the fourth expansion chamber show good agreement with the reference values (grey bars) for all evaluated DFs. Additionally, the flow rate does not have an influence on the dilution performance within a range of 5-20 µL/min. This suggests a good system performance in terms of mixing efficiency and dilution accuracy. However, the colorimetric method is fairly limited in resolution to quantify the dilution accuracy. Therefore a more in-depth analysis is performed based on fluorescence intensity (Section 3.3.1).
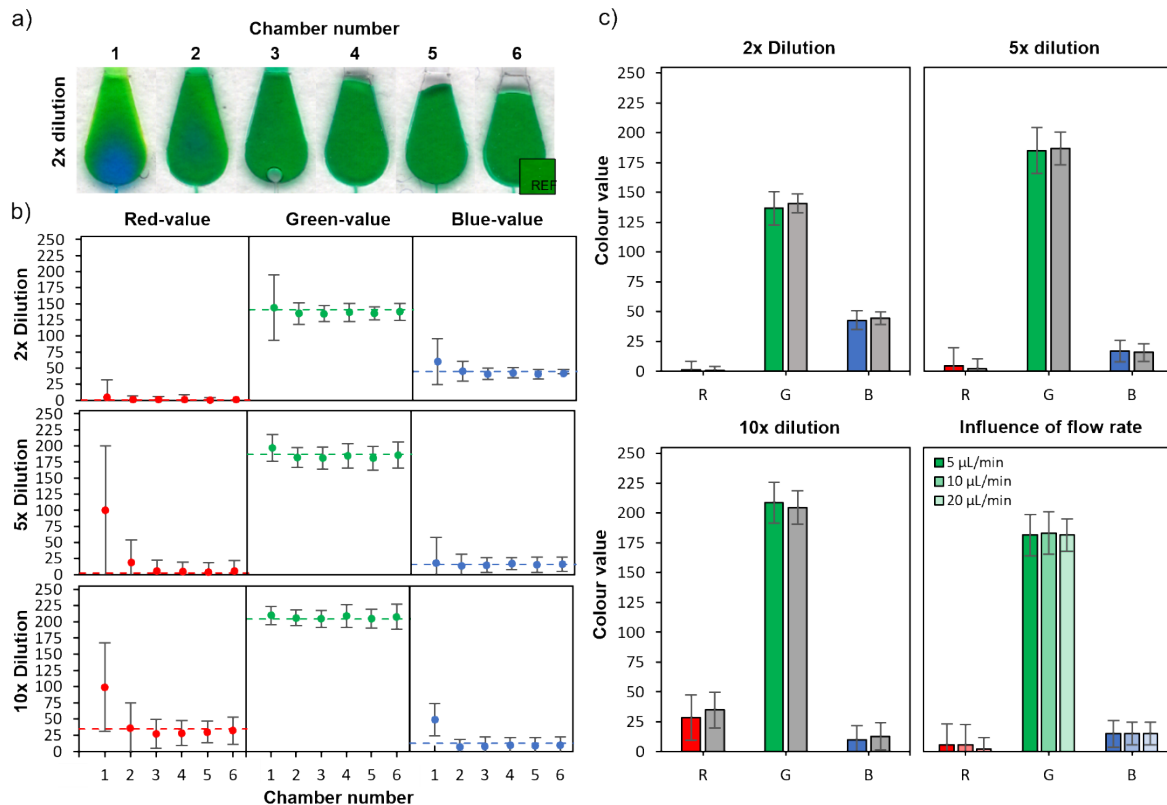
Figure SI. 1: a) Scanned images, illustrating the evolution of the sample-diluent (blue-yellow) plug distribution within each of the six expansion chambers of a dilution module with DF = 2. Reference colour from the manually diluted calibration chip is shown in the right bottom corner. b) Change of mean and distribution of the R, G and B values through the six expansion chambers. Dashed lines represent reference colour values and error bars the standard deviation of the RGB pixel values over the whole chamber (n = ~10.000 pixels per chamber) c) Bar charts representing the mean R, G and B colour value in the fourth expansion chamber for dilution modules with DFs of 2, 5 and 10 run at 10 µL/min and a dilution module with DF of 5 ran at different flow rates of 5, 10 and 20 µL/min. Grey bars illustrate the reference colour values of the manually mixed dilutions. Error bars represent the average (n =3) standard deviation of the colour channel (RGB) within the respective chamber.

SI.2 Non-specific binding of fluorscein proteins

In the characterization experiments for determining the dilution accuracy, a small discrepancy between the undiluted on-chip dilution and undiluted stock fluorescein solution (5 µg/mL) was observed. A potential explanation for this signal drop, is the non-specific binding of the fluorescein proteins to the PVC and PSA walls of the microchannel. To evaluate this, 4 microfluidic channels (channel width of 3mm) were assembled and the fluorescence intensity was measured before and after 10 min incubation with a 25 µg/mL fluorescein solution. In particular, a fluorescent microscope (IX71, Olympus Corporation, Japan) with coupled CCD camera and associated operating software (Hokawo version 2.21, Hamamatsu, Japan) was used to image (2x zoom, 1s exposure time and blue light filter) the empty microchannel (Figure SI. 2a was, left) after which a syringe pump was used to inject a 25 µg/mL fluorescein solution. Upon complete filling, the solution was incubated for 10 minutes and a second microscopic image (Figure SI. 2a was, right) was taken after emptying of the channel at exactly the same position. The average fluorescence intensity profile over the channel width (in the region of interest (ROI), Figure SI. 2a) was then extracted in ImageJ (https://imagej.nih.gov/ij/, USA) for both microscopic images before and after incubation (Figure SI. 2b).

As can be seen in Figure SI. 2a and b, an increase in fluorescence intensity can be noticed which confirms the occurrence of non-specific binding of the fluorescein molecules to the channel walls. The bright intensity in at the side walls, visible in both the microscopic image and the intensity profile, indicate that the non-specific binding phenomena is most prominent at the PSA sidewalls of the microchannel. However, also a significant increase in fluorescence intensity is observed for the PVC surfaces as is illustrated in Figure SI. 2c in which the difference in average fluorescence intensity of the channel region (without channel walls) from 4 independent channels before and after incubation is plotted. The higher level of non-specific binding at the PSA side walls can be a consequence of its more hydrophobic properties (contact angle ~120°) compared to PVC (contact angle ~90°).
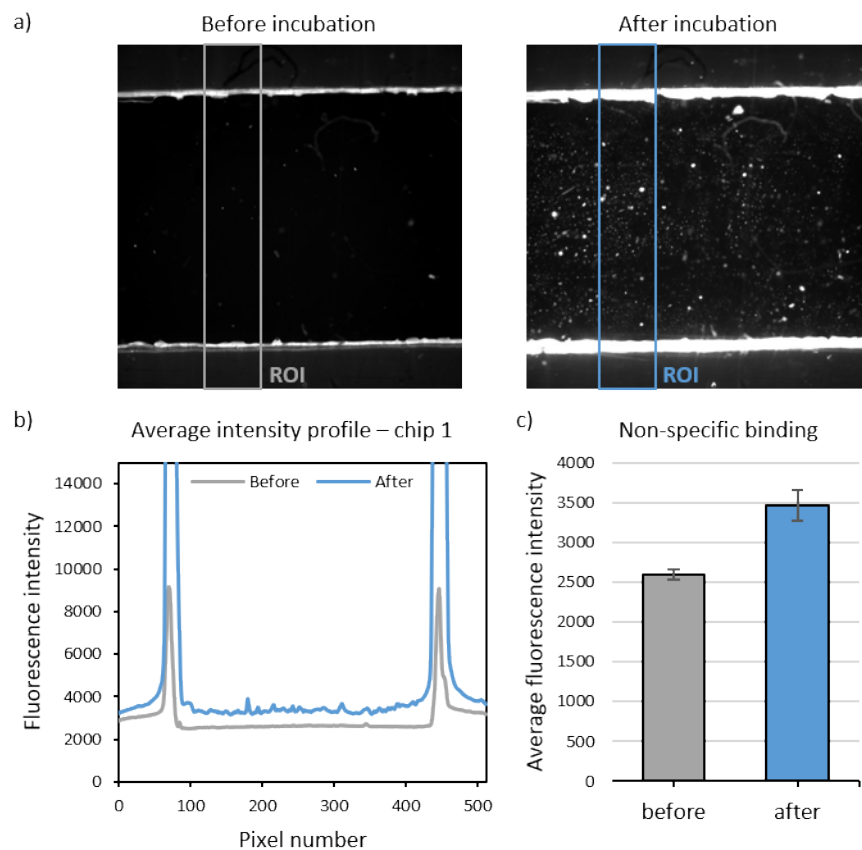

Figure SI. 2: a) Microscopic image (2x zoom) of 3 mm wide microfluidic channel (channel 1) before and after 10 min incubation with 25 µg/mL fluorescein in PBS solution. Grey and blue square represent the ROIs from which the average intensity profiles over the width of the channel is calculated. b) Average fluorescence intensity profiles over the channel width of channel 1 before and after 10 min incubation with 25 µg/mL fluorescein in PBS solution. c) Average fluorescence intensity values of the microfluidic channel (without walls) before and after 10 min incubation with 25 µg/mL fluorescein in PBS solution. Error bars represent 1 standard deviation (n=4).

SI.3 Overview of the microfluidic chip designs

In the figures below, the vectorial designs of the microfluidic chips used for the different experiments within the main manuscript are illustrated. Only the designs for a 5x DF are illustrated as no significant differences in terms of channel dimensions and chip configuration are present for the different DFs.
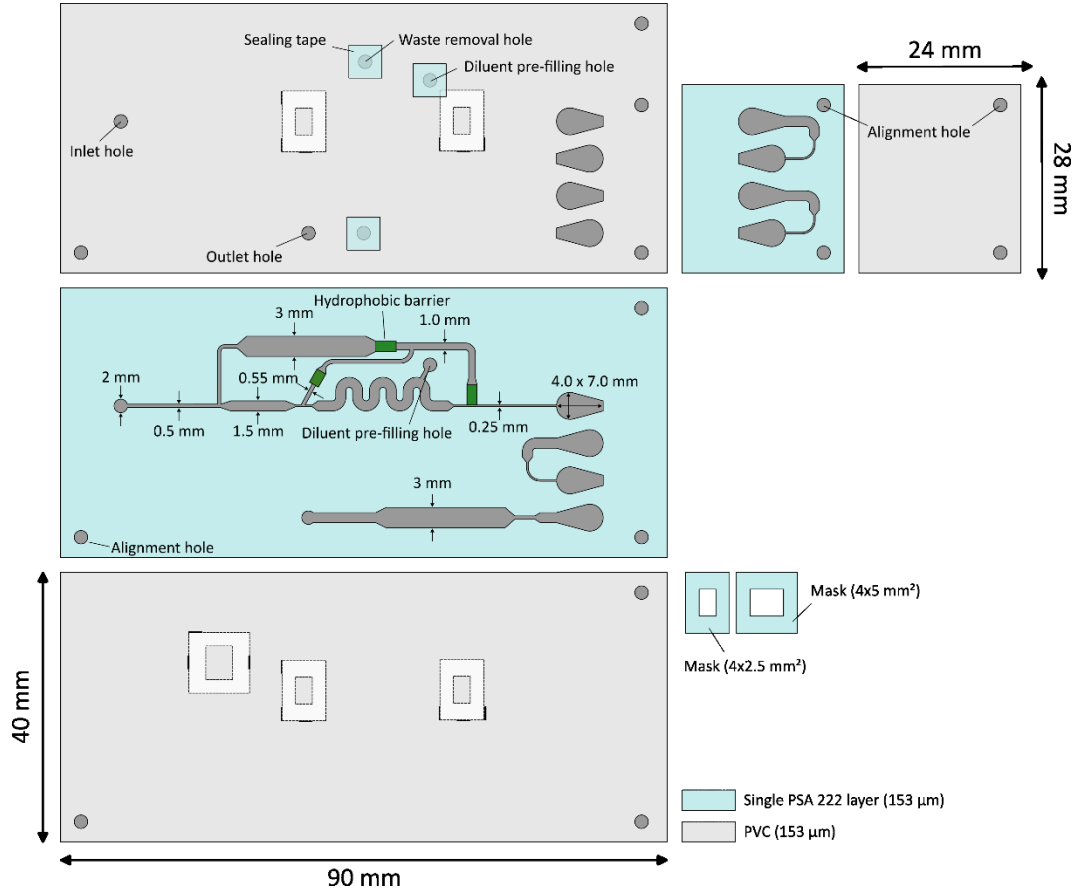

Figure SI. 3: Vectorial design of the different layers comprising the microfluidic chip for single-step dilution (5x DF) accuracy characterization experiments. Dimensions of the whole chip and main microchannels are indicated. Mask positions for local hydrophobic coatings are added to the design of the top and bottom PVC layers. Important to notice is that these masks are removed after the coating step.
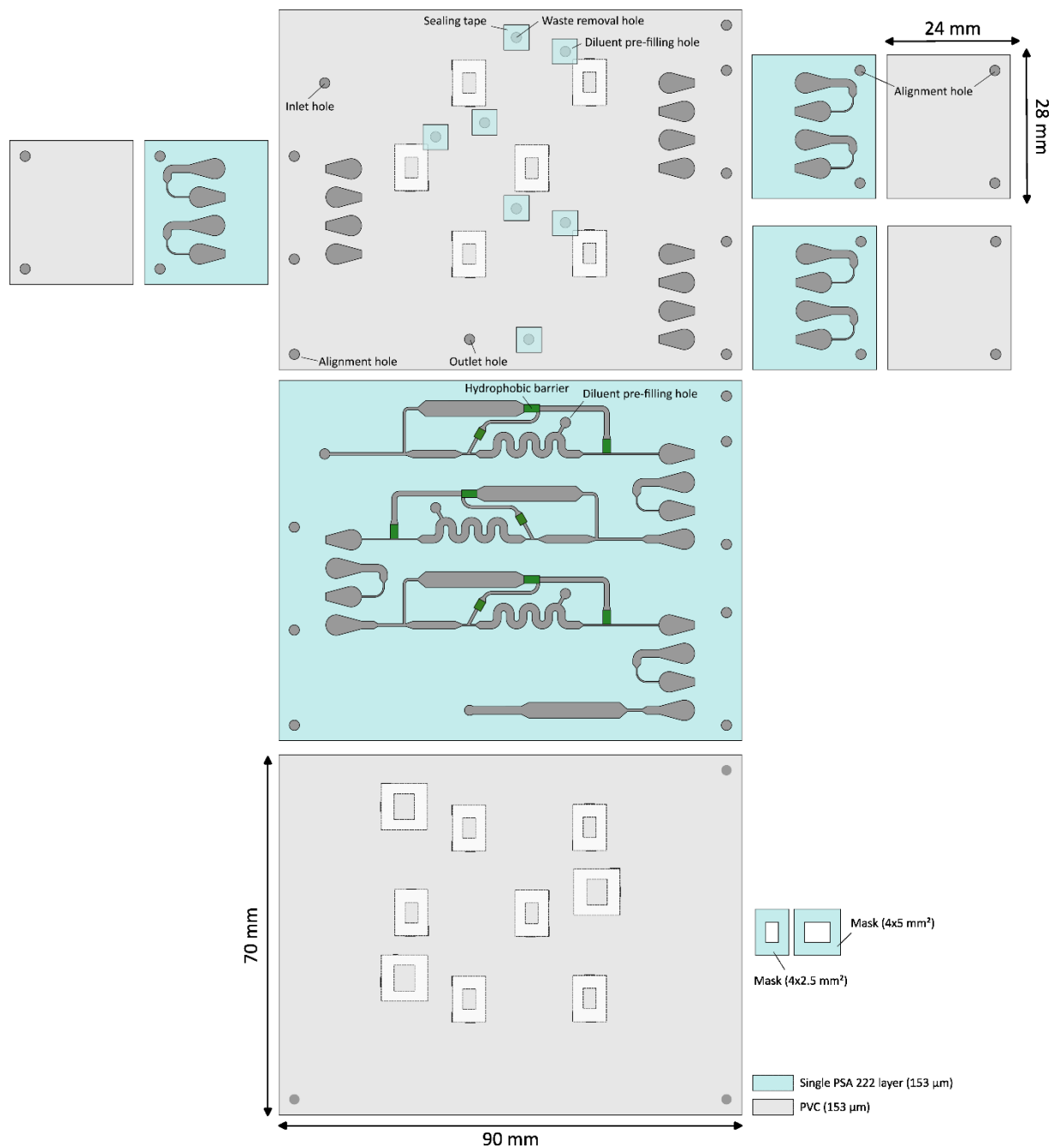
Figure SI. 4: Vectorial design of the different layers comprising the microfluidic chip for serial dilution (125x DF) accuracy characterization experiments. Mask positions for local hydrophobic coatings are added to the design of the top and bottom PVC layers. Important to notice is that these masks are removed after the coating step.
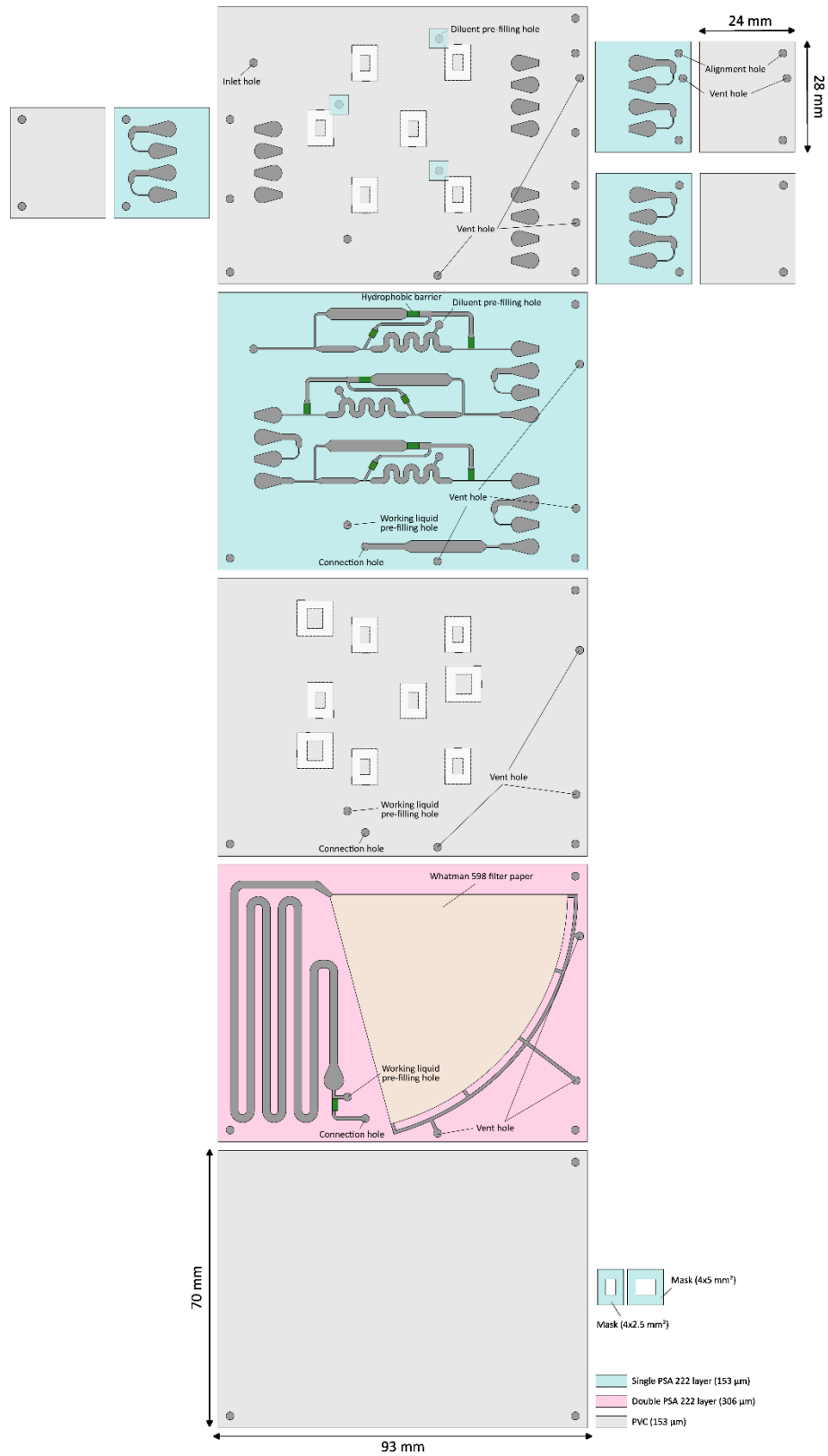
Figure SI. 5: Vectorial design of the microfluidic chip for serial dilution (125x DF) with integrated SIMPLE pump unit. Mask positions for local hydrophobic coatings are added to the design of the top and middle PVC layers. Important to notice is that these masks are removed after the coating step.
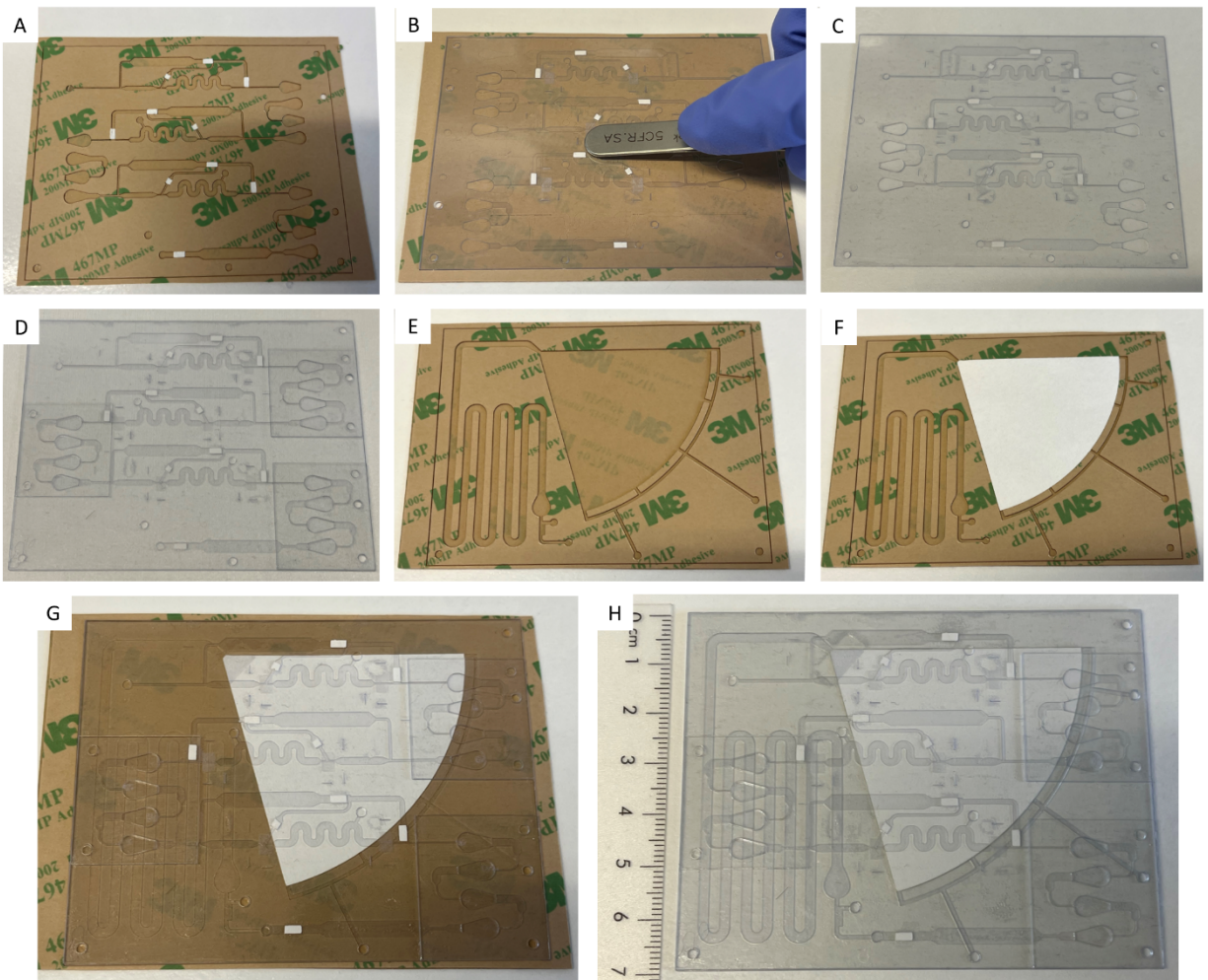
6

Figure SI. 6: Microfluidic chip assembly protocol of a 3-fold log-5 serial dilution chip (125x DF) with integrated SIMPLE pump: A) insertion of hydrophobic barriers in cut out microfluidic network in single PSA 222 layer (after removal of channels), B-C) sealing of the microchannel network with top and bottom PVC films by manual lamination with tweezer (after removal of protective liners), D) addition top part of the 3D expansion chambers to finalize the dilution layer, E-F) insertion of the wedge-shaped filter paper (Whatman grade 598) into the cut out microfluidic network of the pumping layer (double PSA 222 layer, after removal of channels), G) lamination of the dilution layer on top of the pumping layer, followed by sealing with a bottom PVC film. E) Fully-assembled dilution chip, with a ruler to indicate dimensions.

SI. 4 Protocol for microfluidic chip assembly
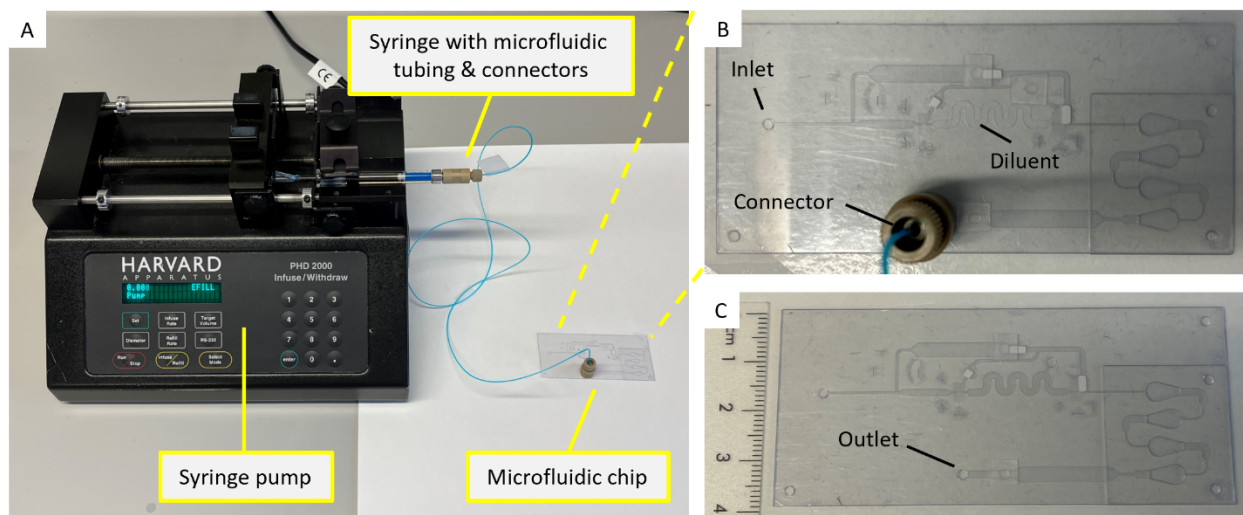
SI.5 Experimental setup

Figure SI. 7: A) Overview of the experimental setup used for optimizing the microfluidic design of the dilution principle and performing all characterization experiments for studying the dilution accuracy and mixing efficiency. A 1 mL syringe was connected to the outlet of the microfluidic chip through microfluidic tubing and attached to a Harvard (PHD 2000) syringe pump. The syringe pump was used to precisely control the flow rate (10 µL/min) inside the microfluidic chip. B) Close-up of the microfluidic chip and the connector used to connect the chip with the microfluidic tubing. A ring of double-sided PSA tape was used to ensure an air-thigh connection. C) Fully-assembled dilution chip, with a ruler to indicate dimensions.